Indian Journal of Engineering & Materials Sciences
Vol. 26, October-December 2019, pp. 369-378

Numerical study on the chip removal and surface quality of CFRP/Ti6Al4V stacks

Jinyang Xu[a]* & Mohamed El Mansori[b]

[a]School of Mechanical Engineering, Shanghai Jiao Tong University, Shanghai 200 240, China
[b]MSMP – EA 7350, Arts et Métiers ParisTech, Châlons en Champagne 510 06, France

Received:13 August 2018; Accepted: 17 July 2019

Machining of multilayer stacks constituted by carbon fibre reinforced polymer (CFRP) composites and titanium (Ti) alloys has been a hot topic receiving extensive attention in both academia and industry due to their superior mechanical properties and widespread applications in the modern aircraft. Compared with the wide availability of experimental studies dealing with the cutting of CFRP/Ti6Al4V stacks, the present work aims to utilize a finite element (FE) method to address fundamentally the machining characteristics of this metallic-composite material. In this paper, a two-dimensional numerical model of orthogonal cutting configuration has been established to improve the mechanism investigations of the bi-material cutting process. The CFRP/Ti6Al4V model has been constructed by establishing three different physical constituents including the Ti phase, the interface and the CFRP phase. Disparate constitutive laws and damage criteria have been implemented to build the anisotropic machinability of the sandwich material. The key cutting phenomena including the chip removal process, machined surface quality and parametric effects on the stack cutting response have been addressed with a particular focus on the quantification of the machining-induced composite damage. The numerical analysis sheds light on several implicit mechanisms dominating the stack machining and offers a better CFRP/Ti6Al4V cutting understanding.

Keywords:- CFRP/Ti6Al4V stacks, Orthogonal cutting, Finite element analysis, Chip formation, Machining damage, Surface quality

1 Introduction

Multilayer stacks made of carbon fibre reinforced polymers (CFRPs) and titanium alloys are becoming increasingly attractive in the modern aerospace industry due to the need to motivate the development of advanced aircraft structures favouring the energy saving[1, 2]. The composite/metal stack aims to combine resistance and improve specific characteristics without significantly increasing the part weight. The compound stacks are often utilized as a good candidate to override standard fibrous composites and individual metal alloys in situations where high thermo-mechanical stresses are applied and specified levels of high performance are required. Despite their widespread use in the industry, CFRP/Ti6Al4V stacks are extremely difficult to machine because of the significant disparity in properties of the involved constituents. For instance, the composite laminate is by nature inhomogeneous that consists of two distinct constituents (abrasive reinforcing fibres and ductile polymer matrix) with completely different properties[3, 4]. By contrast, titanium alloys exhibit poor thermal conductivity, low elastic modulus and high chemical activity, machining of which involves severe phase deformation and transformation occurring in the adiabatic shear band (ASB) and second shear band as reported by Zhu *et al.*[5]. The mentioned characteristics complicate the chip separation process and the defect formation mechanisms of the metallic-composite stacks. In machining CFRP/Ti6Al4V stacks, the specific problems as widely reported in the literature are serious cutting-induced damage, rapid tool wear and short tool life[1, 6-8].

To reveal the underlying cutting mechanisms of this multilayer material, a variety of experimental studies have been performed in recent decades. Ramulu *et al.*[9] were among the earliest to address the machinability issues in drilling Gr/Bi-Ti stacks by using different tool materials. They found that the disparate properties of the stacked constituents significantly affected the tool life and led to the increased matrix degradation and excessive titanium burr formation. The drilling-induced damage became prevalent at the bi-material interface region. Cong *et al.*[10] performed the rotary ultrasonic machining of CFRP/Ti6Al4V stacks using variable and fixed feed rates. The authors stated that using variable feed rates could greatly reduce the cutting force and torque of

*Corresponding author (E-mail: xujinyang@sjtu.edu.cn)

CFRP/Ti6Al4V stacks compared with the use of fixed feed rates. However, the variable feed rates may result in more excessive tool wear, higher surface roughness and larger groove depth than the fixed feed rates under specific cutting conditions. Park *et al.*[11] conducted an experimental study of the wear mechanisms in drilling CFRP/Ti6Al4V stacks when using WC and PCD drills. The results indicated that the abrasive wear caused by the hard carbon fibres and the adhesive wear induced by the titanium adhesion were the key wear modes governing the tool wear progression. The PCD drill yielded a longer tool life than the conventional WC drill, but it underwent chipping fracture because of its inherent brittleness. Ghassemieh[6] studied the cutting performance and wear mechanisms of coated carbide drills in drilling CFRP/Ti6Al4V stacks. The authors pointed out the significant role of tool wear in the force generation, machined surface roughness and induced hole damage. Furthermore, Isbilir and Ghassemieh[7] performed a comparative study of tool life and hole quality when drilling CFRP/Ti6Al4V stacks. The results confirmed that the feed rate affects significantly the drilling forces, the burr formation and the hole surface roughness. The combined wear modes of each phase could significantly shorten the tool life of drills. Zhu *et al.*[12] investigated the effects of different tool geometries in dry drilling of Al/Ti stacks using multipoint, step and double cone drills. The results emphasized the importance of using a functionally-designed tool geometry (*i.e.* a double cone drill) in achieving the excellent surface quality of the cut multilayer stacks. In addition to the above investigations, Xu and El Mansori[13] highlighted the effects of different cutting sequences in drilling CFRP/Ti6Al4V stacks and stated that the titanium chip evacuation could cause severe damage to the composite holes when subjected to the CFRP → Ti drilling sequence. To guarantee excellent machined surface quality, a careful selection of the cutting sequence strategy should be undertaken during the drilling of metallic-composite stacks.

Although the referenced experimental investigations[6,7,9-11,13] have led to a better understanding of machining CFRP/Ti6Al4V stacks, the method used is still time-consuming and requires exhausting tests for the post-process studies of machined surfaces. In contrast, the numerical method is a promising alternative being helpful to improve the mechanism investigations of this bi-material with low costs and high efficiency. However, very limited studies dealing with the numerical investigations of CFRP/Ti6Al4V cutting are reported in the literature. This is due to the difficulty of establishing reliable FE models characterizing the multi-tool-work interaction of the stack machining and the complexity of describing the physical behaviour of the stack interface. In accordance with our previous numerical studies[14, 15], the current paper was an extended investigation to characterize the machined surface morphologies and subsurface damage extents of CFRP/Ti6Al4V stacks with varying cutting conditions via the numerical method. To simplify the complexity of the numerical models, the most-used orthogonal cutting configuration was adopted and an FE model using the concept of the cohesive zone was developed for the CFRP/Ti6Al4V machining. The objective of this paper is to simulate the chip removal process of these metallic-composite stacks and clarify the physical interactions and coupling effects of each stacked phase machining on the resulting stack surface morphologies and subsurface damage. Cutting parameters over a wide range were examined to identify the anisotropic machinability of the sandwich material. The chip separation process, the machined surface quality and the parametric effects on the CFRP/Ti6Al4V cutting response were addressed. The results discussed in this paper allow several guidance to the manufacturing sectors for the high-quality machining of multilayer metallic-composite stacks.

1.1 Assumptions of the present numerical work

Although mechanical drilling is the most-used manufacturing process for metallic-composite stacks due to the need for fastening and riveting assembly, numerical modelling of drilling is rather complicated, time-consuming and shows difficulty to observe the underlying cutting physics in a more clear way. By contrast, the orthogonal cutting can be utilized as an efficient way to inspect the fundamental mechanisms of work materials subjected to various machining processes when several necessary assumptions such as the simplification of the details of the tool-work interaction and the complex tool geometries are considered. To simplify the numerical simulation and consider also the modelling efficiency and accuracy, the orthogonal cutting configuration and the following assumptions were adopted in the present work.

- The FE model of CFRP/Ti6Al4V stacks was developed in a two-dimensional (2D) orthogonal cutting configuration.

- The cutting tool was simplified as a rigid body without any deformation during the cutting process.
- A macro-mechanical model for the stacked CFRP phase was adopted and the composite material was assumed as an equivalent homogeneous material (EHM).

1.2 Numerical setup of the FE model

The present work used the orthogonal cutting method to offer an easy interpretation of mechanisms of drilling CFRP/Ti6Al4V stacks *via* the FE method. The 2D orthogonal cutting model incorporating the fundamental features of a stack drilling process was developed into the Abaqus/Explicit code (Version 6.11). To simulate the stack cutting operation, the machining process was specified in Fig.1. Details of the FE model can be found in the authors' previous studies [14, 16]. The entire cutting model consists of four fundamental physical parts including the tool part, CFRP part, interface and Ti part with a total size of 2 mm ×1 mm (L×H) for the CFRP/Ti6Al4V material. Displacements of the workpiece bottom were fixed in all directions while the left edge was constrained towards the cutting-speed direction (X direction). The cutting tool was driven by a cutting velocity on its reference node to move in the X direction so as to finalize the cutting process. The cutting tool was modelled as a rigid body with defined geometries including a rake angle (α = 0°), a clearance angle (γ = 7°) and an edge radius (r_ε= 2 μm) as depicted in Fig.1. The Ti part was modelled as a fully isotropic and homogeneous material. Linear quadrilateral continuum plane strain elements (CPE4RT) with

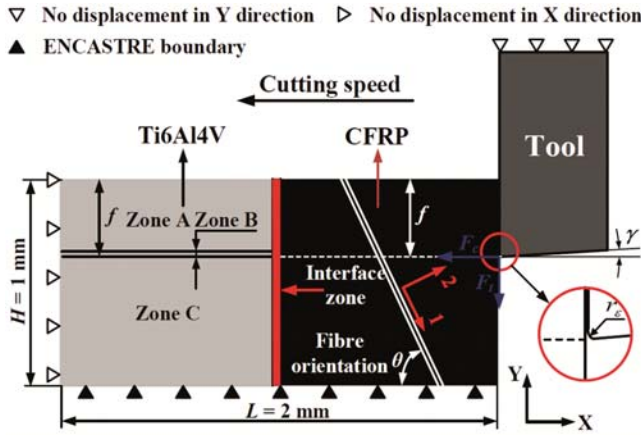

Fig. 1 — A schematic diagram of the established orthogonal cutting model for the CFRP/Ti6Al4V stack (α = 0°, γ = 7° and r_ε = 2 μm)[14, 16]

reduced integration were utilized for a coupled temperature-displacement analysis, and an enhanced hourglass control was selected for the entire set of the Ti elements. The Ti part was separated into three physical zones to optimize the contact management during the FE simulation where zone A denotes the separated chip layer, zone B signifies the predefined separation path and zone C represents the machined titanium surface.

The CFRP composite comprises two distinct phases (reinforcing fibres and polymer matrix) and globally exhibits anisotropic behaviour. However, for simulations in a macro-mechanical model, the material was assumed as an equivalent homogeneous material (EHM). The CFRP part was modelled by using four-node plane-stress linearly interpolated elements (CPS4R) with reduced integration and automatic hourglass control. Note that a plane-strain analysis that is used typically for metal cutting is inappropriate for the machining of FRP laminates due to the extent of out of plane material displacement observed during cutting experiments[17-19]. The fibre orientation defined in the present CFRP model is identical to the intersection angle between the fibre direction and the cutting speed direction as shown in Fig.1. To link the Ti phase and the CFRP phase, an interface layer was built in the FE model having a thickness of approximately 5 μm and simulated as a quick transition zone by using cohesive elements available in the Abaqus/ Explicit code. It should be noted that the interface used here serves as a technical control for the "CFRP-to-Ti" contact management during the numerical simulation. A triangular traction-separation cohesive formulation with linear softening was used to represent its mechanical response.

The interaction between the node sets of the tool surface and the workpiece surface was ruled using the surface-to-surface contact algorithm coupled with a kinematic contact algorithm with the finite sliding formulation. Specifications of penalty contact algorithm and rough friction formulation were defined between the interface-CFRP coupling and the interface-Ti coupling. An additional contact pair was assigned between the CFRP layer and the titanium layer in order to prevent them from penetrating into each other when the interface elements were eroded. Finally, the friction behaviour ruling the tool-work contact pairs was described by Coulomb criteria through the use of friction coefficient.

1.3 Progressive damage models for the CFRP/Ti6Al4V stacks

The studied CFRP/Ti6Al4V stack consists of one Ti6Al4V alloy and one unidirectional (UD) T300/914 laminate. The mechanical/physical properties of the work material can be found in the authors' previous research work[16]. Since the metal alloy exhibits isotropic nature and ductile failure behaviour, the most-used Johnson-Cook (JC) constitutive law and JC damage criteria[20, 21] were adopted to simulate its machining behaviour. The JC law provides a satisfactory description of the behaviour of metals and alloys as it considers large strains, high strain rates and temperature dependent visco-plasticity encountered in machining.

The basic expression of the JC constitutive law is shown as follows:

$$\bar{\sigma} = \underbrace{\left(A + B\bar{\varepsilon}^{n}\right)}_{\text{Strain hardening}}\underbrace{\left(1 + C\ln\left(\dot{\bar{\varepsilon}}/\dot{\bar{\varepsilon}}_0\right)\right)}_{\text{Strain rate sensitivity}}\underbrace{\left\{1 - \left[\left(T - T_r\right)/\left(T_m - T_r\right)\right]^{m}\right\}}_{\text{Thermal softening behaviour}} \quad \ldots (1)$$

where $\bar{\sigma}$ is the equivalent flow stress, $\bar{\varepsilon}$ is the equivalent plastic strain, $\dot{\bar{\varepsilon}}$ is the equivalent plastic strain rate, $\dot{\bar{\varepsilon}}_0$ is the reference equivalent plastic strain rate, T is the workpiece temperature, T_m is the material melting temperature, T_r is room temperature, A, B, C, m and n are material constants.

The JC damage law is expressed as follows:

$$\bar{\varepsilon}_i = \left[D_1 + D_2\exp\left(D_3 \cdot P/\bar{\sigma}\right)\right]\left[1 + D_4\ln\left(\dot{\bar{\varepsilon}}/\dot{\bar{\varepsilon}}_0\right)\right]\left[1 + D_5\left(T - T_r\right)/\left(T_m - T_r\right)\right] \quad \ldots (2)$$

$$\omega = \sum\left(\Delta\bar{\varepsilon}/\bar{\varepsilon}_i\right) \quad \ldots (3)$$

in which $\bar{\varepsilon}_i$ is the equivalent plastic strain at the damage initiation, P is the hydrostatic pressure, $P/\bar{\sigma}$ is the stress triaxiality, $\dot{\bar{\varepsilon}}$ is the equivalent plastic strain rate, $\dot{\bar{\varepsilon}}_0$ is the reference equivalent strain rate, T is the workpiece temperature, T_m is the material melting temperature, T_r is room temperature, D_1-D_5 are the damage parameters, ω is the scalar damage parameter and $\Delta\bar{\varepsilon}$ is the equivalent plastic strain increment.

The simulated composite material was a unidirectional (UD) T300/914 carbon/epoxy laminate. The CFRP laminate was modelled as an EHM by considering its anisotropic behaviour related to the fibre orientation (θ). The definition of the composite fibre orientation (θ) was based on the introduction of the material coordinate system (1, 2) into the CFRP phase as shown schematically in Fig.1. The element erosion of the CFRP phase was defined through the concept of stiffness degradation[22,23]. This means the local material properties (*e.g.* longitudinal modulus and shear modulus) of the examined elements will be reduced when the implemented failure criteria reach the unity during the FE simulation. Hashin damage criteria that show the excellent suitability for the composite cutting modelling were implemented to describe the machining behaviour of the CFRP phase, which consider four fundamental failure modes, *i.e.*, the fibre-tensile failure, the fibre-compression failure, the matrix-tensile failure and the matrix-compression failure. The interface zone was modelled as a quick transition region through the concept of the cohesive zone (CZ). The traction-separation law with linear softening was utilized to simulate its mechanical behaviour. The damage initiation and evolution were controlled using the BK damage law functionally available in the *Abaqus*/Explicit code.

2 Experimental Validation of the Proposed FE Model

Due to the lack of experimental data in the orthogonal cutting of CFRP/Ti6Al4V in the literature, the stack model was validated in terms of individual Ti layer cutting and CFRP layer cutting. Since the interface was modelled as a quick transition zone with a very small thickness, its influences on the machining responses of CFRP/Ti6Al4V could be ignored. Both the CFRP phase model and the Ti phase model were validated rigorously until they were capable of replicating consistent results with the experimental observations extracted from the open literature. For the validation purpose, all the numerical simulations were run under the same cutting conditions as those used in the literature. Details regarding the stack model validation can be found in the authors' previous studies[14, 16].

3 Results and Discussion

3.1 Chip removal process

Machining CFRP/Ti6Al4V exhibits differences from cutting standard composite laminates and individual metal alloys due to the multi-tool-work interaction domain. Generally, the chip removal mechanisms of CFRP/Ti6Al4V can be considered as a combination of brittle fracture and elastoplastic deformation. To inspect the CFRP/Ti6Al4V cutting process, Fig. 2 and Fig. 3 show the chip formation

process in terms of different fibre orientations (θ) under the fixed cutting conditions of v_c= 10 m/min and f = 0.2 mm/rev. It is noted that when the tool edge cuts into the CFRP phase, powdery chips are produced along the tool rake face. For the 0° CFRP phase, the chip formation mechanisms consist of the mode I loading and the fracture along the fibre/matrix interface, the mode II loading through the tool advancement and the fracture perpendicular to the fibre direction under bending loads[19]. The numerical observations are consistent with the reality of CFRP cutting previously reported in the literature[24,25]. Fracture/crack regimes inside the uncut chip layer are observed propagating towards the 0° fibre orientation. This phenomenon can be explained by the fact that the rupture of the fibre/matrix system is governed by a combination of bending-induced shear and compression-induced shear resulting from the tool advancement, which generates the interfacial debonding of the fibre/matrix system towards the fibre-axis direction. As the tool tip cuts into the Ti phase, continuous chips are generally promoted. Note that under the simulated cutting conditions the morphology of the produced Ti chips appears continuous rather than serrated due to the use of an extremely low cutting speed (v_c = 10 m/min) which minimizes the segmentation frequency of the Ti chip removal process. Additionally, the used $v_c \times f$ value (0.002 m^2/min) is much lower than the critical value of 0.004 m^2/min responsible for the occurrence of Ti chip segmentation as stated by several experimental studies[26, 27].

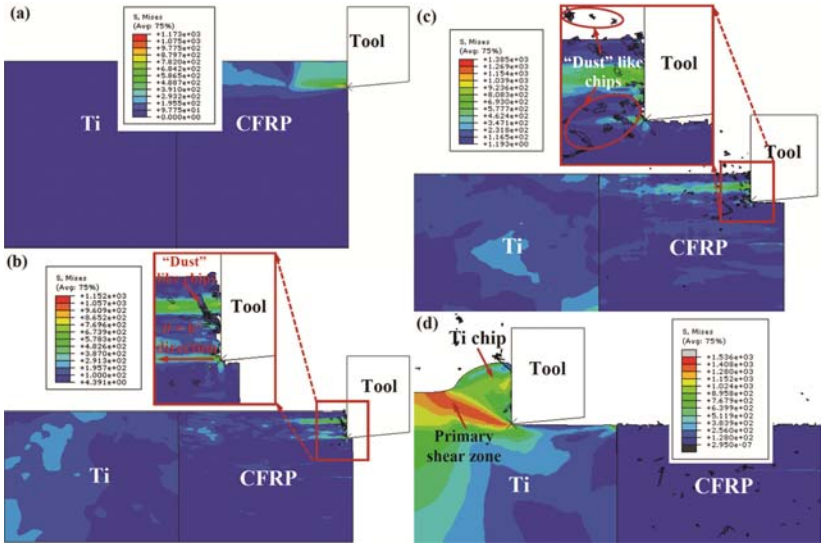

Fig. 2 — Chip formation process in the orthogonal cutting of CFRP/Ti6Al4V stacks (θ = 0°), (a) $t = 6.01 \times 10^{-5}$ s, (b) $t = 2.12 \times 10^{-4}$ s, (c) $t = 7.52 \times 10^{-4}$ s and (d) $t = 9.12 \times 10^{-3}$ s (v_c= 10 m/min and f = 0.2 mm/rev).

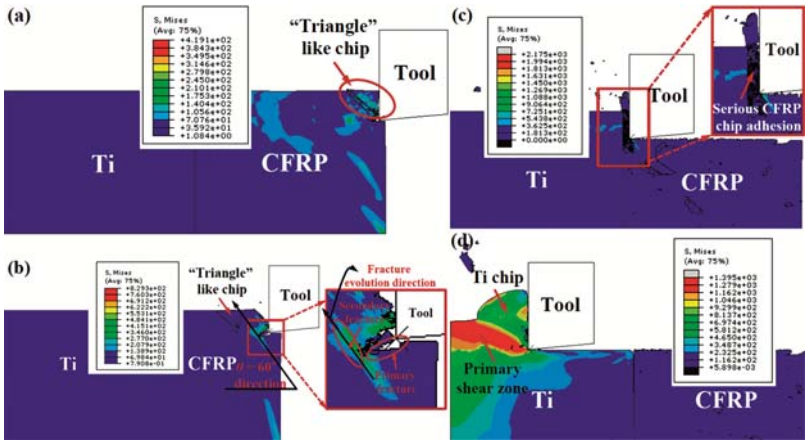

Fig. 3 — Chip formation process in the orthogonal cutting of CFRP/Ti6Al4V stacks (θ = 60°), (a)$t = 2.1 \times 10^{-4}$ s, (b) $t = 6.0 \times 10^{-4}$ s, (c) $t = 5.64 \times 10^{-3}$ s and (d) $t = 9.44 \times 10^{-3}$ s (v_c= 10 m/min and f = 0.2 mm/rev).

In the case of cutting 60° CFRP/Ti6Al4V stacks, both the crack initiation and propagation are observed towards the fibre direction when the tool initially penetrates into the CFRP phase as shown in Fig.3. However, triangular chips are produced which are contrary to the cutting of the 0° CFRP phase. This phenomenon can be attributed to the fact that in cutting CFRP composites with a higher acute fibre orientation the chip formation is induced by a succession of two main fracture mechanisms, namely the primary fracture mode and the secondary fracture mode. As depicted in the magnified view of Fig. 3(b), the primary fracture is initiated by the compression-induced shear perpendicular to the fibre axis while the secondary fracture is characterized by the fibre/matrix debonding along the fibre direction during the tool advancement (θ = 60°). Once the secondary fracture reaches the composite free surface, it results in the complete chip showing a triangular shape. The chip flow in cutting the 60° CFRP phase appears to be governed by the in-plane shear properties of the unidirectional composite laminate. The simulated results match well with the experimental observations of Arola and Ramulu[28]and Iliescu *et al.*[29] as shown in Fig. 4. With the ongoing tool advancement, particularly when the cutting edge approaches the interface zone, the resected CFRP chips are found adhering onto the tool rake face. As the tool fully cuts into the Ti phase, the produced Ti chips exhibit the same morphologies as those observed in the cutting of 0° CFRP/Ti6Al4V stacks.

3.2 Machined surface quality

Machined surface quality plays a key role in the service performance of the stack-made components and consequently determines the final part acceptance. Since the fibre orientation has a significant impact on the cutting behaviour of CFRP/Ti6Al4V stacks, an investigation of machined surface morphologies with different fibre orientations was performed to clarify its effects on the cut surface quality. Figures (5-8) show the gained results under two different fibre orientations of 0° and 60°.

As seen in Figs 5 and 7, the machined surface of the CFRP phase appears much rougher than that of the cut Ti phase regardless of the used fibre orientations. Various micro-cracks, fibre fragments and surface damage are produced within the CFRP surface. In contrast, the machined Ti surface appears much flatter nearly without defects nor cracks. This is attributed to the elastoplastic deformation mode that controls the titanium chip separation, resulting in the continuous chip formation. Consequently, the machined surface is generated much smoother than its counterpart. Furthermore, as shown in the two examined θ configurations, delamination damage is likely to occur towards the stack interface. Increasing the fibre orientation seems to exacerbate the interface delamination extent. For instance, in the orthogonal cutting of a 60° CFRP/Ti6Al4V stack, typically a larger length of delamination damage is promoted at the CFRP/Ti6Al4V interface as shown in Fig. 7. The predicted delamination length (d_m = 80.6 μm) is approximately 2.58 times as long as that (d_m = 31.2 μm) generated under the cutting condition of θ = 0°.

In addition, the machined CFRP surface basically comprises four types of failure including the fibre-compression failure, the fibre-tensile failure, the matrix-compression failure and the matrix-tensile failure as depicted in Figs 6 and 8. To identify the effects of the fibre orientation on the composite-phase damage, the extent of the fibre/matrix damage in each

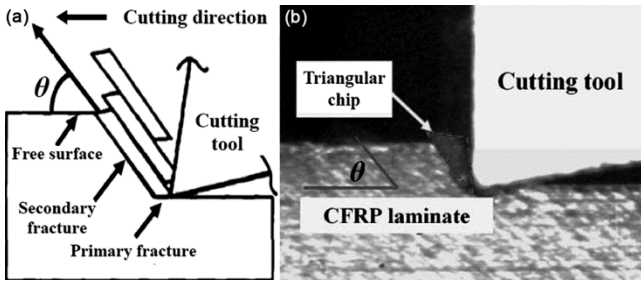

Fig. 4 — Chip formation in the orthogonal cutting of unidirectional fibre reinforced composites with an acute θ angle: (a) a scheme depicting the chip formation of composite laminates from the work of Arola and Ramulu[28]and (b) a high-speed camera image showing the chip separation process of CFRP cutting from the experimental work of Iliescu *et al.*[29]

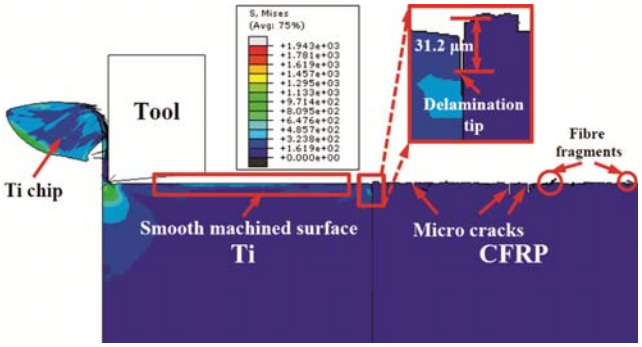

Fig. 5 — Numerical predictions of the machined surface morphology of a CFRP/Ti6Al4V stack with 0° fibre orientation (v_c = 10 m/min and f = 0.2 mm/rev).

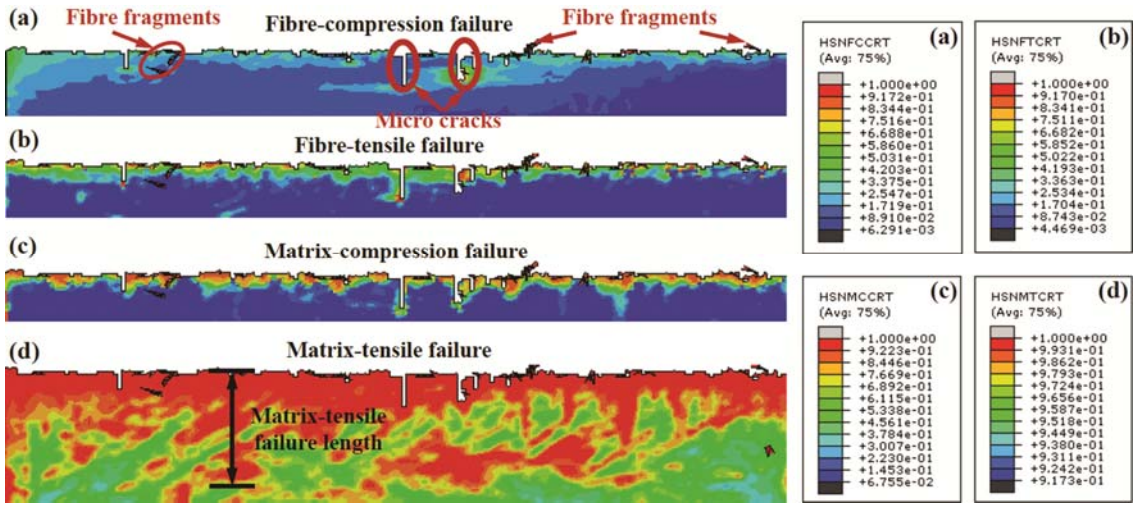

Fig. 6 — Numerical predictions of four types of cutting-induced CFRP damage for 0° fibre orientation (v_c = 10 m/min and f = 0.2 mm/rev), (a) fibre-compression failure, (b) fibre-tensile failure, (c) matrix-compression failure and (d) matrix-tensile failure.

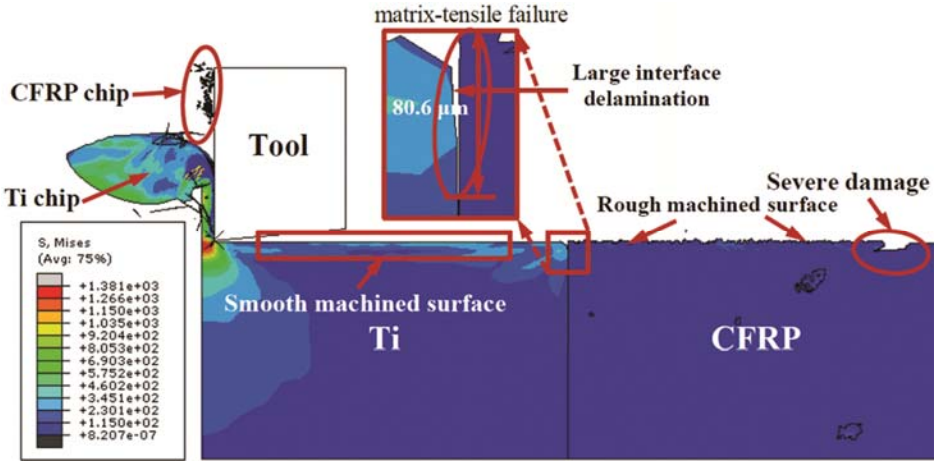

Fig. 7 — Numerical predictions of the machined surface morphology of a CFRP/Ti6Al4V stack with 60° fibre orientation (v_c = 10 m/min and f = 0.2 mm/rev).

type was measured as the maximum length from the machined surface to the deepest damaged zone. Fig. 9 presents the comparative results between θ = 0° and θ = 60°, where FC indicates the fibre-compression failure length, FT denotes the fibre-tensile failure length, MC signifies the matrix-compression failure length and MT represents the matrix-tensile failure length. The fibre orientation is confirmed to have a remarkable influence on the severity of the composite-phase damage. Upon the results in Fig. 9, an elevated fibre orientation often leads to an increased extent of the four types of the fibre/matrix failure. The phenomenon can be explained by the change of mechanisms dominating the chip separation process with respect to the fibre orientation. In the case of cutting a lower θ angle (θ = 0°), the rupture of fibres is caused by a combination of bending-induced and compression-induced shear that generates a rupture plane parallel to the fibre direction. As such, a small area of failure is produced beneath the machined composite surface. In contrast, when machining composites with a higher fibre orientation (θ = 60°), the mechanical bending becomes a dominant chip separation mode, and higher cutting resistance is encountered during the chip removal process. Consequently, a more in depth area of fibre/matrix damage is generated after the completion of machining.

3.3 Parametric effects on the CFRP/Ti6Al4V cutting response

Figures (10-12) show the variations of the cutting force (F_c), the composite-phase damage and the interface delamination with different cutting speeds (v_c), feed rates

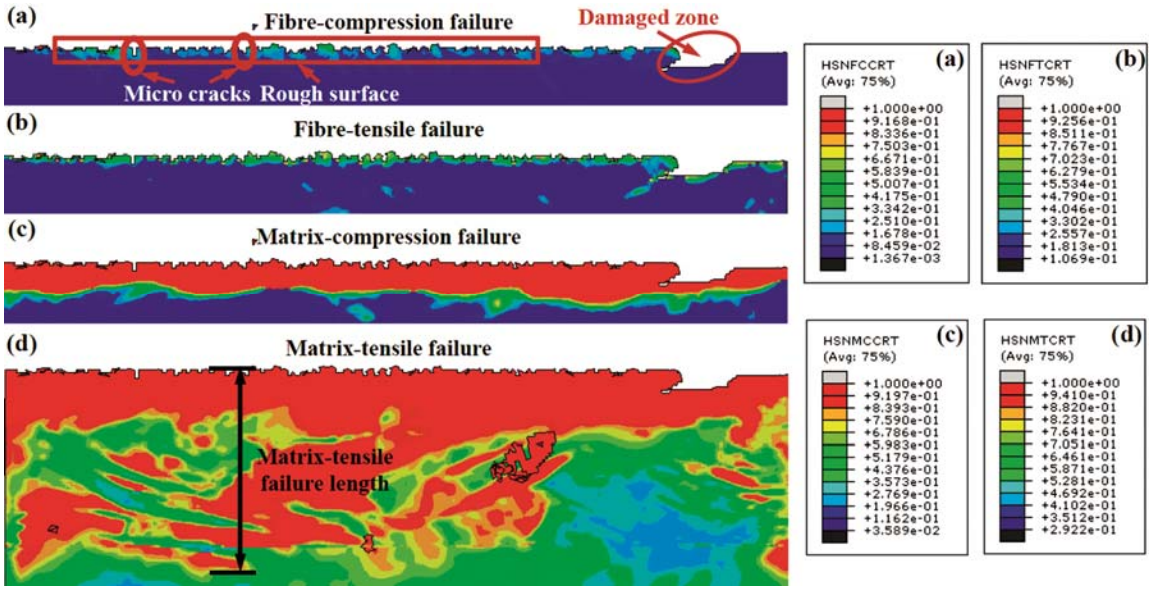

Fig. 8 — Numerical predictions of four types of cutting-induced CFRP damage for 60° fibre orientation (v_c = 10 m/min and f = 0.2 mm/rev), (a) fibre-compression failure, (b) fibre-tensile failure, (c) matrix-compression failure and (d) matrix-tensile failure.

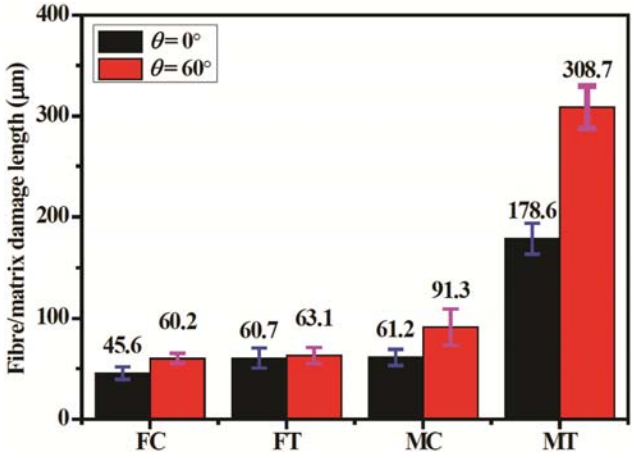

Fig. 9 — Comparative results of the predicted fibre/matrix damage in cutting CFRP/Ti6Al4V with two different fibre orientations of 0° and 60° (v_c = 10 m/min, f = 0.2 mm/rev, FC indicates the fibre-compression failure length, FT denotes the fibre-tensile failure length, MC signifies the matrix-compression failure length and MT represents the matrix-tensile failure length).

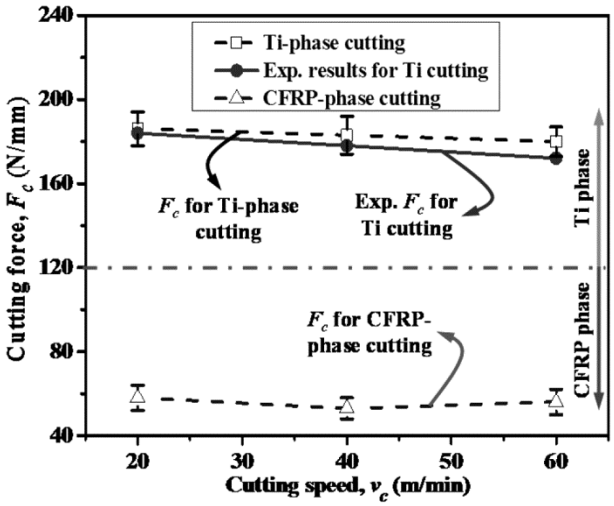

Fig. 10 — Numerical estimations of the effects of the cutting speed (v_c) on the cutting force (F_c) of CFRP/Ti6Al4V stacks (f = 0.1 mm/rev and θ = 0°) (Experimental results for the Ti phase cutting were extracted from Cotterell and Byrne[30]).

(f) and fibre orientations (θ). Note that the simulated force magnitudes (in N/mm) were normalized as the ratio of the average cutting force value to the workpiece thickness. The composite-phase damage was evaluated based on the failure that causes the maximum damage extent of the CFRP phase. The interface delamination extent was measured as the maximum length from the machined surface to the delamination tip as shown schematically in the magnified interface zone of Fig. 5.

As shown in Figs. 10 and 11, it is clear that during the machining of the CFRP/Ti6Al4V stacks, the titanium phase typically produces higher cutting forces than the CFRP phase due to its specific chip separation mode of elastoplastic deformation[32]. In addition, the cutting speed has an insignificant effect on the cutting force, especially for the CFRP-phase machining. This is because the main effects of the cutting speed on the composite cutting forces rely on its thermal softening of the workpiece material. Since the heat generation and the resulting cutting temperatures were ignored in the simulation, the cutting speed shows a negligible effect on the cutting forces of the CFRP phase. The observed phenomenon

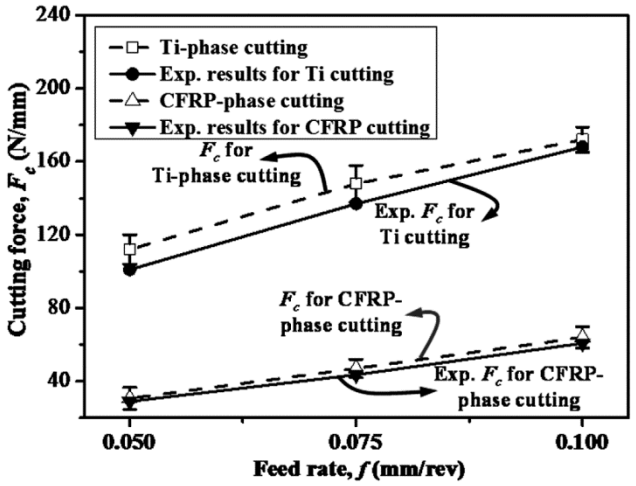

Fig. 11 — Numerical estimations of the effects of the feed rate (f) on the cutting force (F_c) of CFRP/Ti6Al4V stacks (v_c = 60 m/min and θ = 0°) (Experimental results for the Ti phase cutting were extracted from Cotterell and Byrne[30] and experimental results for the CFRP phase cutting were extracted from Iliescu *et al.*[31]).

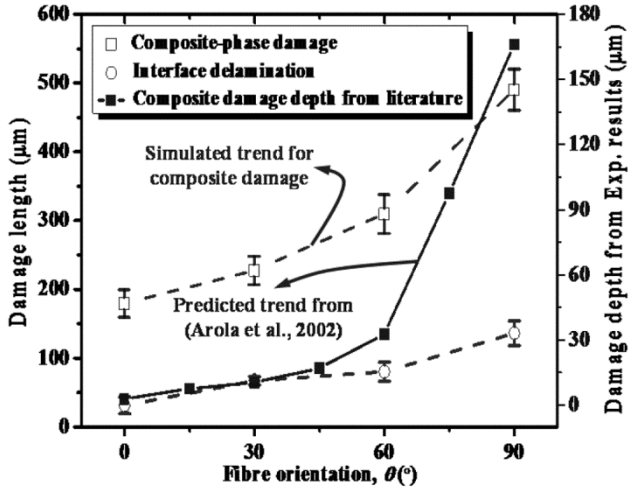

Fig. 12 — Numerical estimations of the effects of the fibre orientation (θ) on the composite-phase damage and interface delamination extents during the orthogonal cutting of CFRP/Ti6Al4V stacks (v_c = 10 m/min and f = 0.2 mm/rev) (Comparative results were extracted from Arola *et al.*[17]).

agrees with the findings of most experimental studies dealing with the drilling of fibrous composites as reported in the review done by Liu *et al.*[33]. When cutting the titanium phase, the F_c magnitudes exhibit an inversely proportional relationship with the cutting speed such that an increased cutting speed leads to a decreased F_c. The phenomenon is attributed to the high cutting temperature promoted at the tool-chip interface that softens the uncut workpiece and thus reduces the cutting resistance. In contrast, the feed rate shows a remarkable impact on the cutting forces of both the Ti phase and the CFRP phase. This is quite understandable that an increase in the feed rate requires the tool to cut off more chip volume per cutting time. As such, a higher cutting force is generated to detach the chips from the workpiece. The simulated F_c magnitudes yield a good agreement with the experimental observations from the literature [30, 31] as shown in Figs 10 and 11, which confirms the credibility of the proposed FE model.

With regard to the cutting-induced damage of CFRP/Ti6Al4V stacks, the fibre orientation is observed to have a clear impact on both the composite-phase damage and the interface delamination as depicted in Fig.12. The phenomenon is related to the varying chip separation mode with the fibre orientation. This is because when increasing the fibre orientation, the CFRP chip separation tends to be dominated by the bending-compression cutting coupled with an out-of-plane shear, which increases the difficulty of the chip breakage and consequently leads to the large damage extent. It should be noted that the findings agree well with the numerical prediction and the experimental measurement from the literature[17,34] during the orthogonal cutting of fibre reinforced composites. In Fig.12, the increasing trend of the numerical predictions for the effects of the fibre orientation on the composite-phase damage also matches well with the predicted trend gained by Arola *et al.*[17]. Moreover, increasing the fibre orientation tends to cause a larger extent of delamination damage as depicted in Fig.12. This can be explained by the fact that when the fibre orientation increases ($0° \leq \theta \leq 90°$), higher cutting forces are generated during the machining of CFRP composites that would make the fracture mode I dominate the failure of the interface region[32]. As a consequence, a larger extent of interface delamination was promoted. The above results suggest that to reduce the subsurface damage, a small fibre cutting angle configuration should be adopted in the machining of CFRP/Ti6Al4V stacks.

4 Conclusions

In this paper, a 2D finite element model was developed to simulate the chip formation during the orthogonal cutting of CFRP/Ti6Al4V stacks. The chip removal process of CFRP/Ti6Al4V stacks was investigated with respect to different fibre orientations. The surface morphologies of the machined stacks were characterized and the cutting-induced damage was quantified. Based on the results acquired, the following conclusions can be drawn:

(i) The cutting mechanisms of CFRP/Ti6Al4V stacks can be considered as a combination of brittle fracture and elastoplastic deformation modes. The resected CFRP chips are small fragments resulting from the fracture along the fibre/matrix interface through cantilever bending and the fracture occurring perpendicular to the fibre axis in the case of $\theta = 0°$. For acute fibre orientations ($\theta = 60°$), the chip separation is dominated by the compression-induced shear perpendicular to the fibre axis followed by the fracture along the fibre/matrix interface during the tool advancement. Moreover, serious composite chip adhesion is found to occur on the tool rake face when the tool cuts across the interface region and subsequently attacks the metallic phase.

(ii) The analysis of the surface quality confirms that the CFRP surface resulting from the stack cutting is much rougher than the cut Ti surface due to the brittle-fracture chip separation mode. Serious micro-cracks, fibre fragments and surface damage are detected on the CFRP surface. The fibre orientation has a significant impact on the cutting-induced damage of the composite phase such that a higher fibre orientation leads to a larger extent of the fibre/matrix failure.

(iii) The parametric study highlights the significant effect of the feed rate on the cutting forces and the vital role of the fibre orientation in the formation of the composite-phase damage and the interface delamination during the machining of CFRP/Ti6Al4V stacks. To reduce the cutting force magnitudes and the cutting-induced damage extents, high cutting speeds, low feed ratesas well as small fibre orientations should be adopted for the machining of CFRP/Ti6Al4V stacks.

Acknowledgement

The authors gratefully acknowledge the financial support of the National Natural Science Foundation of China (Grant No. 51705319).

References

1 Xu J, Mkaddem A & El Mansori M, *Compos Struct,* 135 (2016) 316.
2 Xu J, El Mansori M & Voisin J, *Procedia CIRP*, 46 (2016) 67.
3 Kumar S, Meenu, Satsangi PS & Sardana HK, *Indian J Eng Mater Sci*, 19 (2012) 163.
4 Rajkumar D, Ranjithkumar P & Sathiya Narayanan C, *Indian J Eng Mater Sci*, 24 (2017) 331.
5 Zhu Z, Guo K, Sun J, Li J, Liu Y, Chen L & Zheng Y, *J Manuf Process*, 34 (2018) 531.
6 Ghassemieh E, *Int J Mater Prod Technol*, 43 (2012) 165.
7 Isbilir O & Ghassemieh E, *Mach Sci Technol*, 17 (2013) 380.
8 Wang X, Kwon PY, Sturtevant C, Kim D & Lantrip J, *Wear*, 317 (2014) 265.
9 Ramulu M, Branson T & Kim D, *Compos Struct*, 54 (2001) 67.
10 Cong WL, Pei ZJ, Deines TW, Liu DF & Treadwell C, *Compos Pt B - Eng*, 52 (2013) 303.
11 Park KH, Beal A, Kim D, Kwon P & Lantrip J, *Wear*, 271 (2011) 2826.
12 Zhu Z, Guo K, Sun J, Li J, Liu Y, Zheng Y & Chen L, *J Mater Process Technol*, 259 (2018) 270.
13 Xu J & El Mansori M, *Compos Struct*, 157 (2016) 461.
14 Xu J & El Mansori M, *Int J Precis Eng Manuf*, 17 (2016) 99.
15 Xu J & El Mansori M, *Materials*, 9 (2016) 1.
16 Xu J & El Mansori M, *Int J Adv Manuf Technol*, 87 (2016) 657.
17 Arola D, Sultan MB & Ramulu M, *J Manuf Sci Eng-Trans ASME*, 124 (2002) 32.
18 Hocheng H, Puw HY & Huang Y, *Compos Manuf*, 4 (1993) 103.
19 Wang DH, Ramulu M & Arola D, *Int J Mach Tools Manuf*, 35 (1995) 1623.
20 Johnson GR & Cook WH, In: *Proc of the 7th International Symp on Ballistics*, (1983) 541.
21 Johnson GR & Cook WH, *Eng Fract Mech*, 21 (1985) 31.
22 Lasri L, Nouari M & El Mansori M, *Compos Sci Technol*, 69 (2009) 684.
23 Lasri L, Nouari M & El Mansori M, *Wear*, 271 (2011) 2542.
24 Koplev A, Lystrup A & Vorm T, *Compos*, 14 (1983) 371.
25 Mkaddem A, Ben Soussia A & El Mansori M, *Wear*, 302 (2013) 946.
26 Bayoumi AE & Xie JQ, *Mater Sci Eng A*, 190 (1995) 173.
27 Barry J, Byrne G & Lennon D, *Int J Mach Tools Manuf*, 41 (2001)1055.
28 Arola D & Ramulu M, *Int J Mech Sci*, 39 (1997) 597.
29 Iliescu D, Gehin D, Iordanoff I, Girot F & Gutiérrez ME, *Compos Sci Technol*, 70 (2010) 73.
30 Cotterell M & Byrne G, *CIRP Ann - Manuf Technol*, 57 (2008) 93.
31 Iliescu D, Gehin D, Nouari M & Girot F, *Int J Mater Prod Technol*, 32 (2008) 118.
32 Xu J & El Mansori M, *Int J Precis Eng Manuf*, 16 (2015) 2091.
33 Liu D, Tang Y & Cong WL, *Compos Struct*, 94 (2012) 1265.
34 Wang XM & Zhang LC, *Int J Mach Tools Manuf*, 43 (2003) 1015.